The Astronomical Journal, 153:27 (8pp), 2017 January doi:10.3847/1538-3881/153/1/27

THE INCLINATION OF THE PLANETARY SYSTEM RELATIVE TO THE SOLAR EQUATOR MAY BE EXPLAINED BY THE PRESENCE OF PLANET 9

Rodney Gomes[1], Rogerio Deienno[2,3], and Alessandro Morbidelli[4]
[1] Observatório Nacional Rua General José Cristino 77, CEP 20921-400, Rio de Janeiro, Brazil; rodney@on.br
[2] Laboratoire Lagrange, UCA, OCA, CNRS, Nice, France
[3] Instituto Nacional de Pesquisas Espaciais, São José dos Campos, SP, Brazil
[4] Laboratoire Lagrange, UMR7293, Université Côte dAzur, CNRS, Observatoire de la Côte dAzur, France
Received 2016 July 12; revised 2016 September 19; accepted 2016 September 19; published 2016 December 22

ABSTRACT

We evaluate the effects of a distant planet, commonly known as planet 9, on the dynamics of the giant planets of the solar system. We find that the dynamics of the giant planets can be decomposed into a classic Lagrange–Laplace dynamics relative to their own invariant plane and a slow precession of said plane relative to the total angular momentum vector of the solar system, including planet 9. Under specific configurations for planet 9, this precession can explain the current tilt of $\sim 6^\circ$ between the invariant plane of the giant planets and the solar equator. An analytical model is developed to map the evolution of the inclination of the inner giant planets' invariant plane as a function of the planet 9's mass and orbital elements, and numerical simulations of the equations of motion are performed to validate our analytical approach. The longitude of the ascending node of planet 9 is found to be linked to the longitude of the ascending node of the giant planets' invariant plane, which also constrains the longitude of the node of planet 9 on the ecliptic. Some of the planet 9 configurations that allow the explanation of the current solar tilt are compatible with those proposed to explain the orbital confinement of distant Kuiper Belt objects. This work gives an elegant explanation for the current tilt between the invariant plane of the inner giant planets and the solar equator and also adds new constraints to the orbital elements of planet 9.

Key words: celestial mechanics – planets and satellites: dynamical evolution and stability – Sun: general

1. INTRODUCTION

The gradual discovery of increasingly distant trans-Neptunian objects (TNOs) has allowed new tests for the existence of a yet undiscovered distant planet in the solar system. Gomes et al. (2015) analyzed the large semimajor axis centaurs and concluded that they are produced continually by the decrease of perihelia of scattered disk objects, induced by the perturbation of a distant planet. Trujillo & Sheppard (2014), as they announced the discovery of the distant TNO 2012 VP113, also noted that distant TNOs not perturbed by close encounters with Neptune show a remarkable alignment of their arguments of perihelia and proposed that a distant planet is responsible for this alignment. Madigan & McCourt (2016) argued that gravitational forces in a disk of objects in eccentric orbits can lead to clustering in their pericenters, with no need to invoke a planetary perturber. Their model requires a mass of about 1–10$M_\oplus$ for the disk, which is beyond the best estimates for the scattered disk and inner Oort cloud. Moreover they do not account for the perturbation of the major planets that should induce a spread of the longitudes of perihelia and nodes.

More recently, Batygin & Brown (2016) studied more deeply the orbital alignment of those distant TNOs, showing that the six most distant objects also exhibit a clustering in their longitudes of node; they estimated a probability of 0.007% that this double alignment in argument of perihelion and longitude of the node is just fortuitous. Moreover, they showed that a planet 9 (hereafter named just pl9) could account for said alignment if it had a mass of about 10$M_\oplus$ and an orbit with a semimajor axis between 300 and 900 au, a perihelion distance between 200 and 350 au, and an orbital inclination of about 30° to the ecliptic plane. The Batygin–Brown approach based on secular dynamics is able to determine an approximate orbit for the distant planet that could explain the said alignment, but not the planet's position on that orbit. Fienga et al. (2016) use a typical orbit among those proposed by Batygin & Brown (2016) and determined the range in true longitude of pl9 on that orbit that decreases the residuals in the INPOP ephemerids of Saturn, relative to the Cassini data. Holman & Payne (2016) obtained a similar result using JPL ephemerids. Brown & Batygin (2016) refined their previous results by further constraining the mass and orbital elements of pl9 that are compatible with the observed TNOs orbital alignment. They now argue for pl9's semimajor axis in the range of 380–980 au, perihelion distance in the range of 150–350 au, and a mass between 5 and 20$M_\oplus$, for an orbital inclination of 30°. Malhotra et al. (2016) looked for extra constraints on the pl9 orbit by analyzing the orbital periods of the four longest period TNOs. Their approach is based on the supposition that pl9 is in mean motion resonances with those TNOs. Beust (2016), on the other hand, showed that a mean motion resonant configuration may not be necessary to explain the orbital confinement.

Here we study the precession of the plane orthogonal to the total angular momentum of the four giant planets due to the perturbation of pl9. We find that, given the large distance of pl9, the dynamics of the giant planets can be decomposed into a classic Lagrange–Laplace dynamics relative to their own invariant plane (the plane orthogonal to their total angular momentum vector, hereafter, named iv4) and a slow precession of said plane relative to the total angular momentum vector of the solar system, including pl9. Planetary system formation predicts that planets are formed from a disk of gas and dust and this disk rotates on the same plane as the star's equator. The final planetary orbits, if no mutual close encounters take place, must be approximately coplanar and coincident with the star's equator. We thus suppose that the giant planets and the solar

equator were initially on the same plane. We assume that pl9 was scattered away from the region of the other giant planets when the disk was still present and the solar system was still embedded in a stellar cluster (Izidoro et al. 2015). The stellar cluster is needed, so that the perihelion of the orbit of pl9 can be lifted and pl9 can decouple from the other planets (Brasser et al. 2008). Because most of the angular momentum is in the protoplanetary disk, it is likely that the ejection of pl9 onto an inclined orbit did not significantly change the inclination of the disk and of the other giant planets. For instance, considering a primordial solar disk of 0.005 $M_\odot$, with surface density varying as $1/r$ up to 40 au, we find a total angular momentum for the disk of $0.16\,M_\odot$ au^2 yr^{-1}. Pl9's just-scattered orbit (before perihelion raising by an external force) with semimajor axis at 700 au and perihelion distance at ∼10 au implies an angular momentum of $0.0008\,M_\odot$ au^2 yr^{-1} in absolute value but tilted 30° with respect to the disk. Conservation of angular momentum implies that the old disk angular momentum must equal the vectorial sum of pl9's angular momentum at its just-scattered position and the new disk angular momentum. Triangle geometry allows the computation of the tilt between the old and the new disk of just $\sim 0\overset{\circ}{.}14$. Notice also that the inclination of pl9 might have been increased by the action of the cluster, while lifting the perihelion in a Lidov–Kozai-like dynamics (Brasser et al. 2008). In this case, the increase in pl9 inclination would have no consequences on the inclination of the disk. If instead the ejection of planet 9 from the inner planetary region occurred when the disk of gas had been already substantially removed, the comparison with the total angular momentum of the Jupiter–Neptune system ($\sim 0.02\,M_\odot$ au^2 yr^{-1}) suggests that these planets would also have been perturbed off-plane significantly, implying a tilt of $\sim 1\overset{\circ}{.}2$ for the giant planets if they are tilted together, but the main effect would go to the planet mostly responsible for scattering pl9, possibly Jupiter. However, we consider this case less likely because we expect that, by the time most of the gas disk was removed, the stellar cluster in which the Sun formed would also have dispersed significantly (see, however, Adams et al. 2006). In this case, pl9 could not have been trapped on an orbit with $a \sim 1000$ au; it could have been trapped only on an Oort cloud-like orbit with an ∼10 times larger semimajor axis. Thus, we assume that, at the removal of the protoplanetary disk and of the birth cluster of the Sun, the four major giant planets were on orbits near the solar equator, while pl9's orbit was off-plane. At this point, a slow precession of iv4 started to take place relative to the total angular momentum vector of the solar system, including pl9, keeping, however, the orientation of the solar equator plane unchanged. Thus the current angle between the solar equator and iv4 (about 6°—see below) must be a signature of pl9 perturbation and we aim to find ranges of orbital elements and mass for pl9 that can explain quantitatively the present tilt of iv4 relative to the solar equator.

The solar equator with respect to the ecliptic is identified by an inclination of $I_S = 7\overset{\circ}{.}2$ and a longitude of the ascending node $\Omega_S = 75\overset{\circ}{.}8$ (Beck & Giles 2005). The invariant plane with respect to the ecliptic is defined by an inclination $I_i = 1\overset{\circ}{.}58$ and a longitude of the ascending node $\Omega_i = 107\overset{\circ}{.}58$ (Souami & Souchay 2012). Employing two rotations, we can find the invariant plane angles with respect to the solar equator to be $I_v = 5\overset{\circ}{.}9$ and $\Omega_v = 171\overset{\circ}{.}9$. We will use these parameters throughout the rest of the paper. We also consider that iv4, as above defined, is equivalent to the invariant plane of the solar system mentioned in the works above, which also take into account the inner planets.

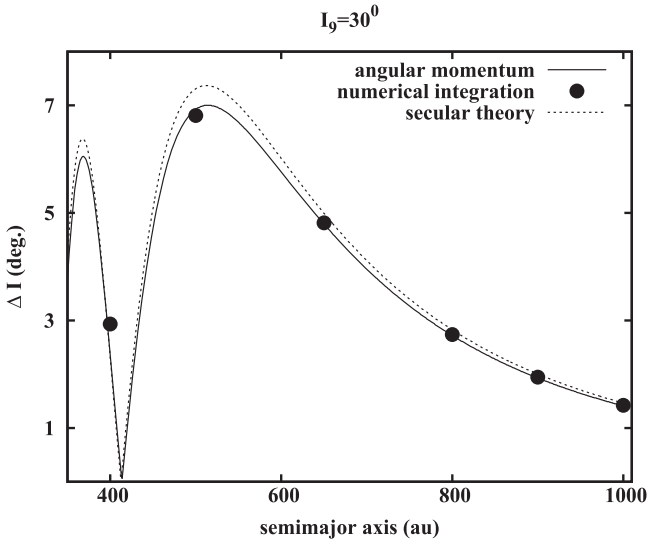

Figure 1. Inclination of iv4 relative to the initial plane (the solar equator) after 4.5 Gy due to the presence of pl9 with $e_9 = 0.7$, as a function of pl9's semimajor axis. The dashed curve shows the prediction from the secular theory described in Section 2.1 and the solid curve from the analytic theory described in Section 2.2. The dots show the results of six numerical simulations that contain no approximations.

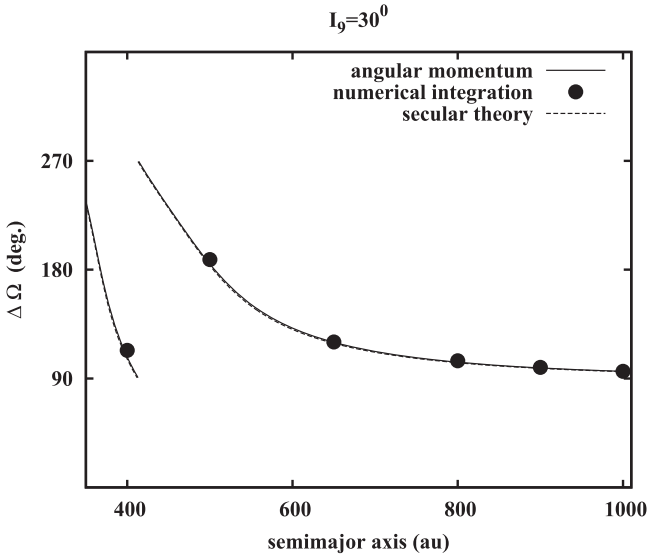

Figure 2. Same as Figure 1 but for the longitude of the node of iv4 relative to the solar equator. Here the two analytic approaches look indistinguishable.

In Section 2, we develop two analytical approaches aimed at determining the tilt experienced by iv4 due to the perturbation of pl9. We also perform some numerical integrations of the full equations of motion to validate our analytical approaches. In Section 3, we apply our analytical method to determine the range of masses and orbital elements of pl9 that can account for the observed tilt of iv4 to the solar equator plane. In Section 4, we draw our conclusions.

2. METHODS

We first apply the classical Laplace–Lagrange formalism up to second order in the inclination to evaluate the variation of the inclination experienced by iv4 due to pl9. Since a second-

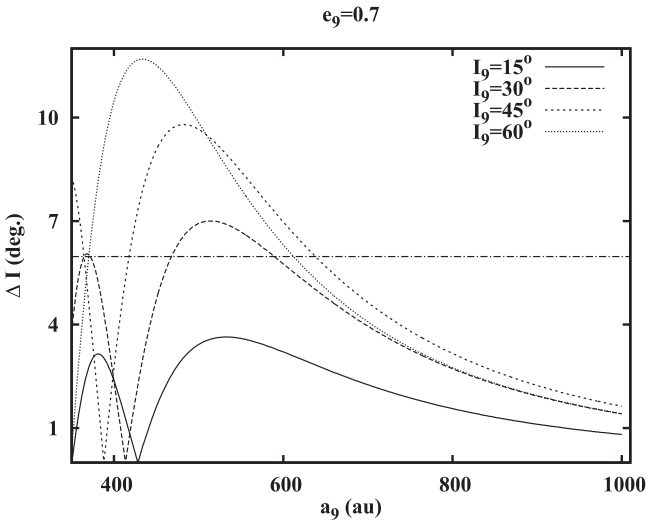

Figure 3. Inclination gained by iv4 with respect to the initial reference frame believed to coincide with the current solar equator for different semimajor axes and initial inclinations of pl9, assuming a mass of $3 \times 10^{-5} M_{\odot}$ and an eccentricity of 0.7. The horizontal line stands for the current inclination of iv4 with respect to the solar equator.

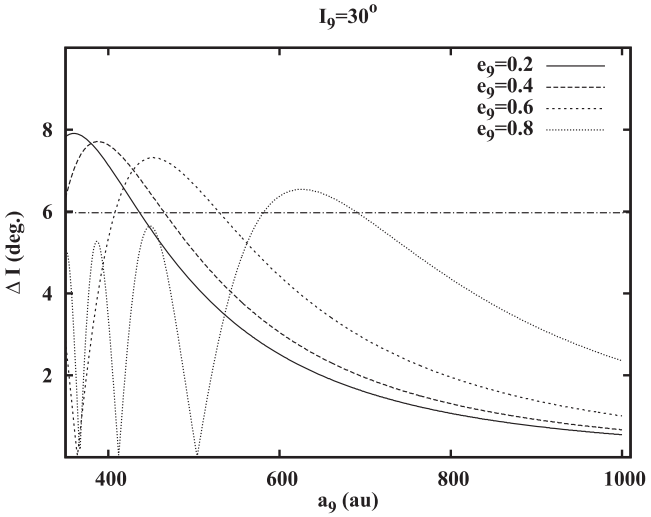

Figure 4. Same as Figure 3, but for different eccentricities and semimajor axes of pl9, assuming an inclination of 30°.

order approach may not be sufficient for large inclinations of pl9, we develop another approach based on the angular momenta of pl9 and the four giant planets. In this case, we make no approximation on the inclinations but just a first-order approximation in the ratio of the known planets' semimajor axes to that of pl9.

2.1. First Approach: Secular Perturbations to Second Order

Following Batygin et al. (2011), we derive a secular theory of the evolution of the inclination of iv4 based on the classical Laplace–Lagrange theory up to the second order in the inclinations. From Murray & Dermott (1999), we have the following form for the classical Hamiltonian:

$$H = \frac{1}{2} \sum_{j=1}^{N} \sum_{k=1}^{N} B_{jk} I_j I_k \cos(\Omega_j - \Omega_k) \tag{1}$$

where j and k indicate the perturbed and the perturbing bodies respectively. The Nth index refers to pl9. All inclinations are expressed with respect to the solar equator, believed to be the initial fixed reference frame. The coefficients B_{jj} and B_{jk} assume the form

$$B_{jj} = -\frac{n_j}{4} \sum_{k=1, k\neq j}^{N} \frac{m_k}{M_{\odot} + m_j} \alpha_{jk} \bar{\alpha}_{jk} b^{(1)}_{3/2}(\alpha_{jk})$$
$$B_{jk} = \frac{n_j}{4} \frac{m_k}{M_{\odot} + m_j} \alpha_{jk} \bar{\alpha}_{jk} b^{(1)}_{3/2}(\alpha_{jk}) \tag{2}$$

where $M_{\odot}$ is the mass of the Sun, m_j and m_k are the masses of the interacting bodies, and n_j is the mean motion of the planet j. $\alpha_{jk} = a_j/a_k$ and $\bar{\alpha}_{jk} = \alpha_{jk}$ for $a_j < a_k$. For $a_j > a_k$, we have $\alpha_{jk} = a_k/a_j$ and $\bar{\alpha}_{jk} = 1$. $b^{(1)}_{3/2}(\alpha_{jk})$ is the Laplace coefficient of the first kind (Murray & Dermott 1999, Ch. 7).

In the context of the Laplace–Lagrange secular theory, valid for small values of the inclination and eccentricity, if we want to account for large values of the inclination and eccentricity of pl9, we need to add some new ingredients to the classical theory. In this manner, the inclination of pl9 was accounted for by reducing pl9's mass by a factor of $\sin I$, i.e., $m_{9_{(\mathrm{new})}} = m_{9_{(\mathrm{real})}} \cos I_9$. By doing this, we consider only the projection of the mass of pl9 onto the planet's reference frame (iv4) (Batygin et al. 2011). As for the eccentricity of pl9, assuming that one cannot derive a simple secular approach (Murray & Dermott 1999), it becomes necessary to somehow incorporate the averaged effect of an eccentric orbit upon the motion of the perturbed planet. According to Gomes et al. (2006), the averaged effect can be computed assuming that the perturber is on a circular orbit of radius b, where $b_9 = a_9\sqrt{1 - e_9^2}$ is the semi-minor axis of the real perturber's orbit. Thus, in order to compute the possible large eccentricity of pl9, we will assume $b_9 = a_9\sqrt{1 - e_9^2}$ to be its circular semimajor axis analog.

Therefore, with the implementations of $m_{9_{(\mathrm{new})}} = m_{9_{(\mathrm{real})}} \cos I_9$ and $b_9 = a_9\sqrt{1 - e_9^2}$, it is possible to rewrite the Hamiltonian (1) in terms of the vertical and horizontal components of the inclination ($p_j = I_j \sin\Omega_j$ and $q_j = I_j \cos\Omega_j$), where the first-order perturbation equations ($\dot{p}_j = \partial H/\partial q_j$ and $\dot{q}_j = -\partial H/\partial p_j$) lead to an eigensystem that can be solved analytically (Murray & Dermott 1999, Ch. 7)

$$p_j = \sum_{k=1}^{N} I_{jk} \sin(f_k t + \gamma_k)$$
$$q_j = \sum_{k=1}^{N} I_{jk} \cos(f_k t + \gamma_k) \tag{3}$$

with f_k being the set of N eigenvalues of matrix $\boldsymbol{B}$ (Equation (2)), I_{jk} the associated eigenvector, and γ_k a phase angle determined by the initial conditions. This leads to the final solution of

$$I_j = \sqrt{p_j^2 + q_j^2}$$
$$\Omega_j = \arctan\left(\frac{p_j}{q_j}\right). \tag{4}$$

Finally, starting with Jupiter, Saturn, Uranus, and Neptune in the equatorial plane of the Sun, given the orbital parameters of

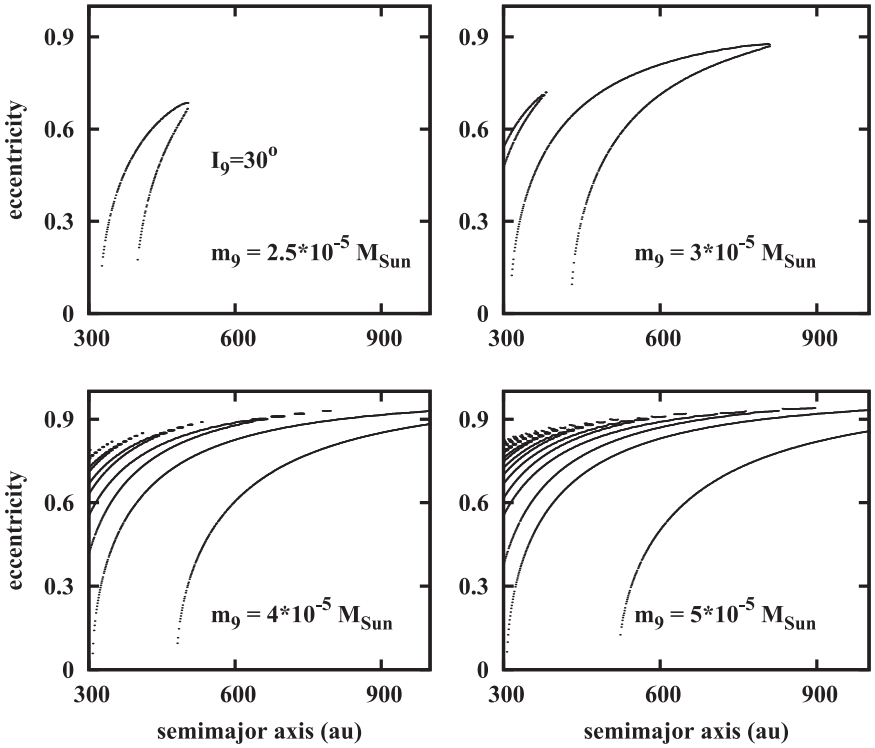

Figure 5. Semimajor axis vs. eccentricity of pl9s that yield a tilt of 5°.9 to iv4 with respect to the solar equator, for $I_9 = 30°$.

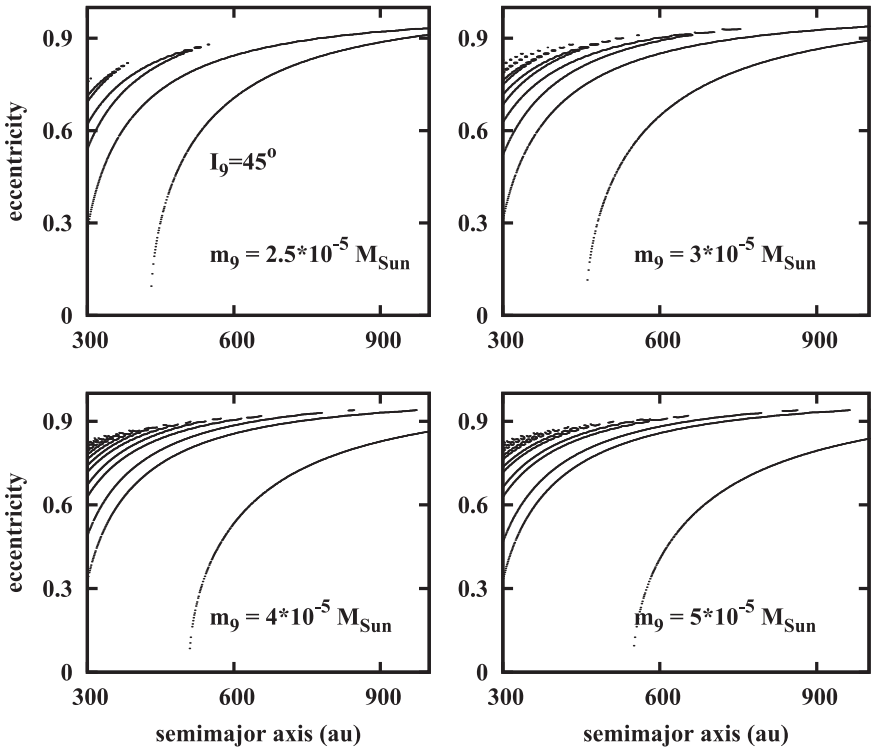

Figure 6. Same as Figure 5, but for $I_9 = 45°$.

pl9, one can verify that the eigenvectors (I_{j5}, $j = 1 \ldots 4$) have the same magnitude. In this way, the equations in (4) also represent the evolution of the pair (I, Ω) of iv4. Despite the modifications we introduced to account for the large inclination and eccentricity of pl9, our method has limitations, being less accurate for large values of I_9 and e_9.

2.2. Second Approach: Angular Momentum

The equation of motion of a planet around a star perturbed by a second planet in a reference frame centered in the star is

$$\ddot{\boldsymbol{r}} = -G(m_9 + M)\frac{\boldsymbol{r}}{r^3} + Gm_9\left\{\frac{\boldsymbol{r}_{19}}{r_{19}^3} - \frac{\boldsymbol{r}_9}{r_9^3}\right\} \qquad (5)$$

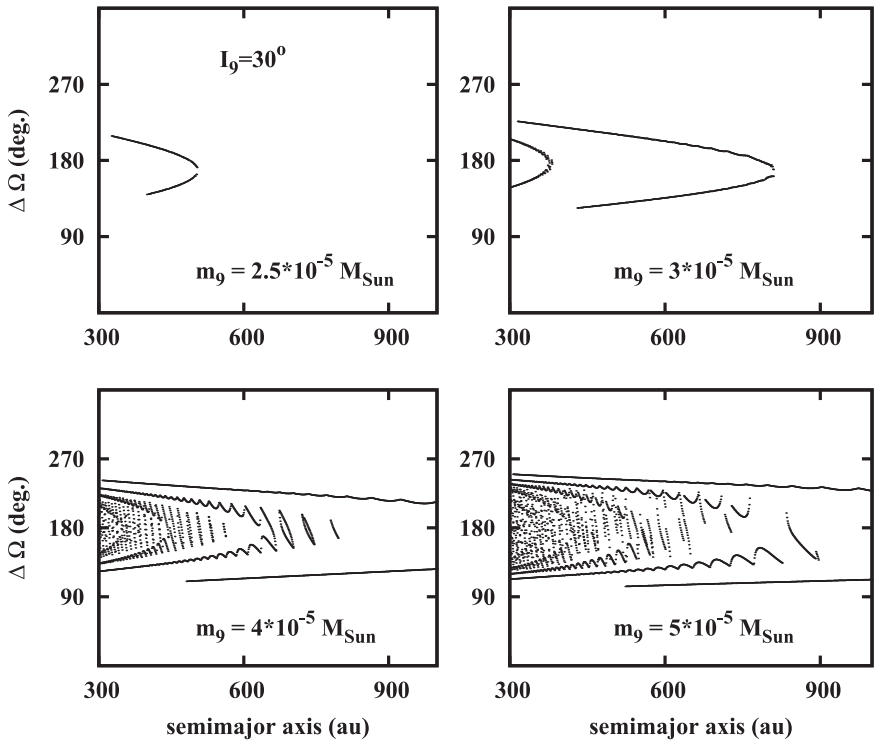

Figure 7. Semimajor axis vs. Ω of pl9s that yield 5.°9 inclination tilt to iv4 with respect to the solar equator, for $I_9 = 30°$.

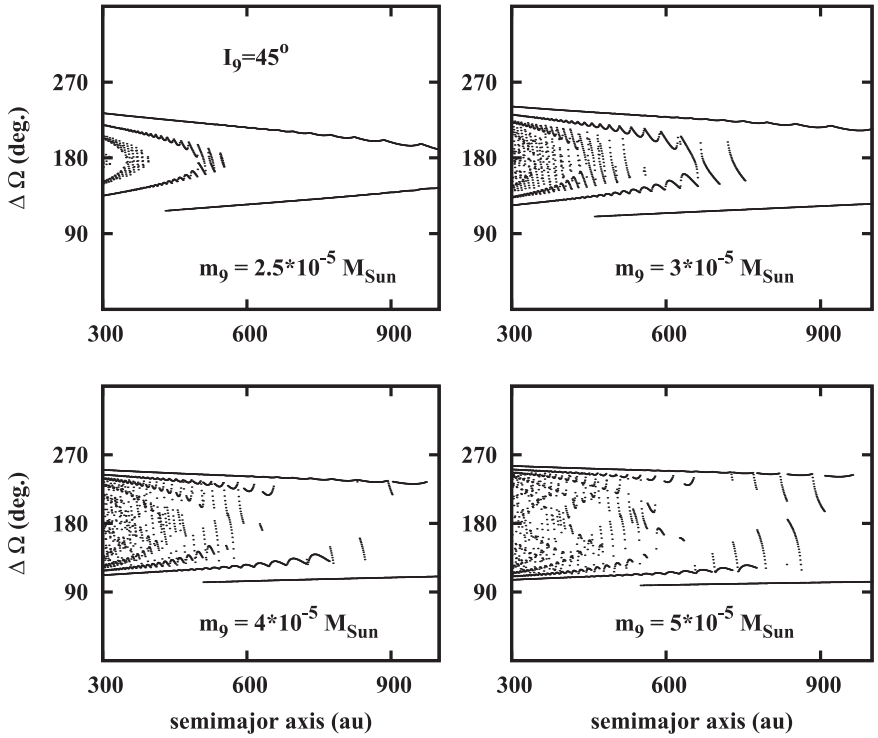

Figure 8. Semimajor axis vs. Ω of pl9s that yield 5.°9 inclination tilt to iv4 with respect to the solar equator, for $I_9 = 45°$.

where the subscript 9 refers to the perturbing planet and the perturbed planet has no subscript. In this equation, $\boldsymbol{r}$ is the radius vector and r is its absolute value, m_9 is the perturbing planet mass, M is the star's mass, G is the gravitational constant, and r_{19} is the distance between both planets. Let us define the angular momentum per unit mass by $\boldsymbol{h} = \boldsymbol{r} \times \dot{\boldsymbol{r}}$. Using Equation (5), the time derivative of $\boldsymbol{h}$ can be found as

$$\dot{\boldsymbol{h}} = \left\{ Gm_9 \frac{\boldsymbol{r} \times \boldsymbol{r}_{19}}{r_{19}^3} - Gm_9 \frac{\boldsymbol{r} \times \boldsymbol{r}_9}{r_9^3} \right\}. \quad (6)$$

Since $\boldsymbol{r}_{19} = \boldsymbol{r}_9 - \boldsymbol{r}$ and $\boldsymbol{r} \times \boldsymbol{r} = 0$, we have to deal just with the vectorial product $\boldsymbol{r} \times \boldsymbol{r}_9$ in Equation (6). We now want to

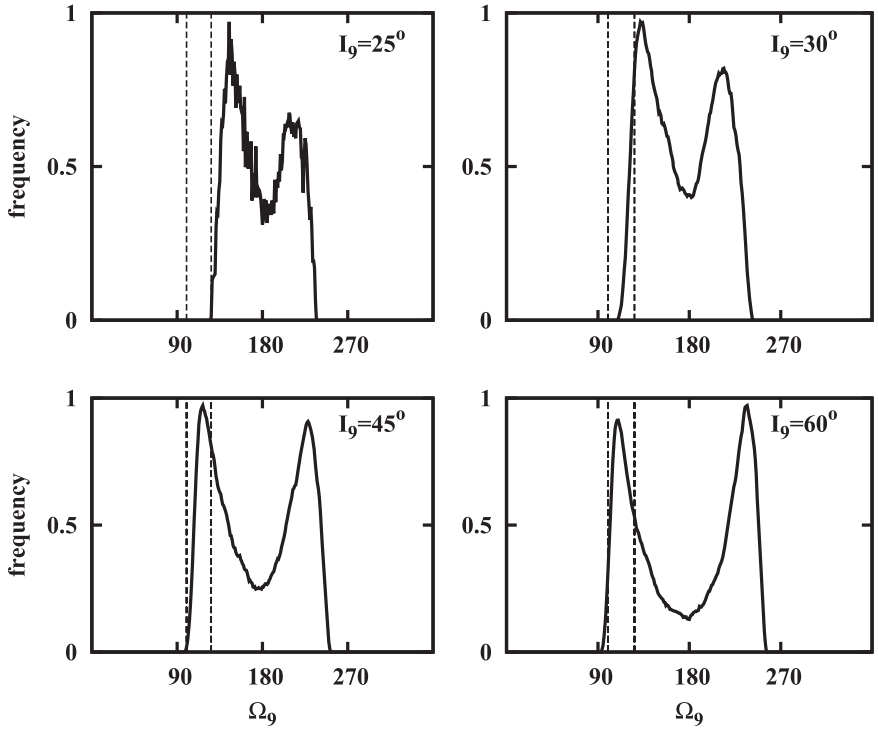

Figure 9. Frequency of possible longitudes of the ascending node on the ecliptic that pl9 must have to yield 5°9 tilt with respect to iv4, for four different inclinations for pl9. Each panel includes masses of pl9 from $2 \times 10^{-5} M_{\odot}$ to $5 \times 10^{-5} M_{\odot}$ with increments of $10^{-5} M_{\odot}$. The vertical lines depict the range of Ω's determined by Batygin & Brown (2016; 113° ± 13°).

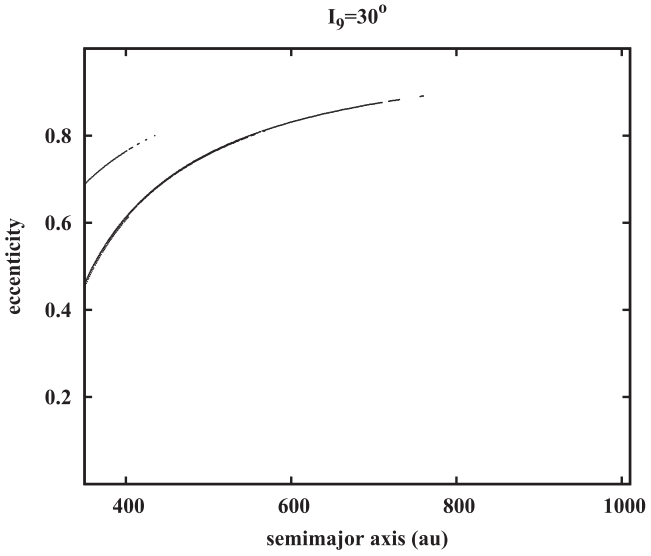

Figure 10. Semimajor axis vs. eccentricity of pl9s that yield a tilt of 5°9 to iv4 with respect to the solar equator, for $I_9 = 30°$, and contrained by the range of longitude of nodes predicted by Batygin & Brown (2016).

average the right hand of Equation (6) in the fast variables for both planets. For that, we suppose two reference frames defined on each of the planets' orbits making an angle I between them. The frames are defined by $(\boldsymbol{i}, \boldsymbol{j}, \boldsymbol{k})$ and $(\boldsymbol{i}_9, \boldsymbol{j}, \boldsymbol{k}_9)$, unitary vectors, where the component $\boldsymbol{j}$ is common to both frames. $\boldsymbol{j}$ is in the intersection of the orbital planes and lies on the invariant plane defined by both planets; $\boldsymbol{i}$ and $\boldsymbol{i}_9$ are orthogonal to $\boldsymbol{j}$ on each of the orbital planes and $\boldsymbol{k}$ and $\boldsymbol{k}_9$ completes the reference frames through the right hand rule. It must be noted that these frames are defined just to compute the derivative of $\boldsymbol{h}$ on those components instantaneously. We now assume that the perturbed planet has a small enough eccentricity so as to consider its orbit as circular. On the other hand, the perturbing planet will be considered eccentric. In this manner, we can represent the radius vector of each of the planets as

$$\boldsymbol{r} = (a \cos l)\, \boldsymbol{i} + (a \sin l)\, \boldsymbol{j} \tag{7}$$

$$\boldsymbol{r}_9 = (r_9 \cos \theta_9)\, \boldsymbol{i}_9 + (r_9 \sin \theta_9)\, \boldsymbol{j}, \tag{8}$$

where a is the perturbed planet semimajor axis, l is the perturbed planet mean longitude, and θ_9 is the angle from the intersection of the planes to the perturbing planet's position, which is the sum of pl9's true anomaly f_9 and the longitude of the ascending node with respect to the invariant plane.

We now put together Equations (6)–(8) and develop the vectorial products remembering that $\boldsymbol{i} \times \boldsymbol{i}_9 = -\sin I \boldsymbol{j}$, $\boldsymbol{i} \times \boldsymbol{j} = \boldsymbol{k}$, $\boldsymbol{j} \times \boldsymbol{i}_9 = -\boldsymbol{k}_9 = -\sin I \boldsymbol{k} + \cos I \boldsymbol{i}$, and $\boldsymbol{j} \times \boldsymbol{j} = 0$. Developing the components in $\boldsymbol{i}$ and $\boldsymbol{k}$, we notice that there is always a trigonometric function in at least one of the fast angles to an odd power, which results in a null average for these components.

For the $\boldsymbol{j}$ component, after developing the vectorial product to the first order in a/r_9, we obtain

$$(\boldsymbol{r} \times \boldsymbol{r}_9)/r_{19}^3 = -(a\ r_9 \cos l \cos \theta_9 \sin I)\ r_9^{-3}\ T \tag{9}$$

where,

$$T = 1 - \frac{3}{2}\frac{a^2}{r_9^2} + 3\frac{a}{r_9}\,(\sin l \sin \theta_9 + \cos l \cos \theta_9 \cos I).$$

The first-order approximation can be quite accurate when a/r_9 is small, which is the case of a distant planet perturbing a close-in one. Averaging in the fast angles l and f_9, which

appears in θ_9 and r_9, for one orbital period, we arrive at

$$\frac{1}{PP_9}\int_0^P\int_0^{P_9}\frac{\boldsymbol{r}\times\boldsymbol{r}_9}{r_{19}^3}\,dt^2=\frac{3}{8}a^2b_9^{-3}\sin 2I \tag{10}$$

where P and P_9 are the orbital periods of the perturbed and perturbing planets, respectively, and $b_9=a_9\sqrt{(1-e_9^2)}$ is the semi-minor axis of the perturbing planet. The term $(\boldsymbol{r}\times\boldsymbol{r}_9)/r_9^3$ averages to zero in all components. The variation of $\boldsymbol{h}$ becomes

$$\dot{\boldsymbol{h}}=\frac{3}{8}G\,m_9\,a^2b_9^{-3}\sin 2I\boldsymbol{j}. \tag{11}$$

Through the way the reference frames were constructed, we have shown that $\boldsymbol{h}$ has only, and always, a non-zero time derivative in the direction of the intersections of the orbital planes. Since the choice of the reference frames could be for any time, we conclude that at any time the non-zero component of the time derivative of $\boldsymbol{h}$ is orthogonal to $\boldsymbol{h}$ on the intersection of the orbital planes. This is satisfied only if the projection of $\boldsymbol{h}$ on the invariant plane is a circle around the origin. The radius of the circle α (where $\sin\alpha=H_9/H_t\sin I$) is the angle between $\boldsymbol{h}$ and $\boldsymbol{H}_t$ where $\boldsymbol{H}_t=m\boldsymbol{h}+\boldsymbol{H}_9$ is the total angular momentum and $\boldsymbol{H}_9=m_9\boldsymbol{r}_9\times\dot{\boldsymbol{r}}_9$ is pl9 angular momentum. The precession frequency is the coefficient multiplying $\boldsymbol{j}$ in Equation (11) divided by $2\pi\alpha h$, where h is the absolute value of $\boldsymbol{h}=\sqrt{GM_\odot a}$.

This approach to compute the variation of the inclination and node of a planet perturbed by another one can be extrapolated to the case of a distant planet perturbing several close-in planets. We noticed by numerical integrations that this approach is accurate enough for the solar system giant planets perturbed by a distant planet, when we replace the four planets by only one with a semimajor axis at 10.227 au and the same angular momentum as the resultant angular momentum of the giant planets.

2.3. Comparison of Both Approaches with Numerical Integrations

We considered the current orbital elements of the four giant planets and a pl9 and ran a numerical integration of the full equations of motion for 4.5 Gy. We noticed that iv4 behaved the same way as if all planets started on the same plane. Thus, for simplification, we started new integrations with the current giant planet's orbital elements except for the inclinations, which were started at zero, and these integrations were used for the comparisons below. We ran a total of six different numerical integrations with different semimajor axes for pl9.[5] The planet's mass and other orbital elements are $m_9=3\times10^{-5}M_\odot$, $e_9=0.7$, $I_9=30^\circ$, $\Omega_9=113^\circ$, $\omega_9=150^\circ$ (Batygin & Brown 2016). Figures 1 and 2 show the comparison of the two analytic approaches with the numerical integrations. We notice good agreement, thus, from now on, we will consider the angular momentum approach to make our analysis.

[5] We also ran one numerical integration with all eight planets and confirmed that the orbital plane of the inner ones just precessed around a common plane, which, in this case, would be an iv8 very close to iv4.

3. CONSTRAINING A PLANET 9 THAT YIELDS A 5°.9 TILT

Figures 3 and 4 show how the inclination of iv4 after 4.5 Gy depends on orbital elements of the perturbing planet. Here we fixed the mass of pl9 at $3\times10^{-5}M_\odot$. The largest value of ΔI in each of these figures stands for the case where the angular momenta of pl9 and iv4 turn 180° around one another. For smaller semimajor axes of pl9, more than one cycle is accomplished by the pair of angular momentum vectors.

The plots in Figures 3 and 4 allow us to compute pl9 parameters that yield an ∼5°.9 inclination between the solar equator and iv4 after 4.5 Gy. for instance, Figure 3 reveals that a planet with $3\times10^{-5}M_\odot$, an eccentricity of 0.7, and a semimajor axis of 600 au has to have an initial inclination of 30° relative to the solar equator to cause the observed tilt. Figures 5 and 6 show the loci of pl9 semimajor axis and eccentricity that yield a tilt of 5°.9 of iv4 relative to the solar equator for four possible masses for the distant planet and two initial values of pl9 inclination. We notice that for a mass $2.5\times10^{-5}M_\odot$ and $I_9=30^\circ$, there are just a few choices of planets that can yield a 5°.9 tilt. A mass as small as $2\times10^{-5}M_\odot$ is unable to yield the right tilt for iv4 if $I_9=30^\circ$. For higher inclinations of pl9, it is possible for iv4 to achieve a tilt of 5°.9 for somewhat smaller masses of the perturber. The constraints on pl9 orbit that we obtain here have similarities with those obtained by Batygin & Brown (2016) using considerations of the orbital alignment of TNOs; though, we usually determine a higher eccentricity for a given semimajor axis. For example, the standard pl9 in Batygin & Brown (2016) with $m_9=10M_\oplus$ and $I_9=30^\circ$ has $a_9=700$ au and $e_9=0.6$. In our case, for the same m_9, I_9, and a_9, the eccentricity must be 0.8. In Brown & Batygin (2016), the best pl9 for $I_9=30^\circ$ and $m_9=10M_\oplus$ has $a_9=600$ au and $e_9=0.5$. In our analysis, for the same I_9, m_9, and a_9, the eccentricity must be 0.71. On the other hand, Malhotra et al. (2016) determined eccentricities lower than 0.4 for $a_9=665$ au; however, in this case, for a coplanar configuration of pl9 with the TNOs.

As iv4 and pl9 orbital planes evolve, their intersections of the solar equator plane define a difference of longitudes of ascending nodes on that plane. Figures 7 and 8 show, respectively, for $I_9=30^\circ$ and $I_9=45^\circ$, pl9 semimajor axis and longitude of the ascending node (Ω) that yield 5°.9 for iv4, on the solar equator plane, with respect to iv4 longitude of the ascending node at 4.5 Gy. This is also shown for four possible masses of the distant planet. We see that iv4 and pl9 are on average opposed by 180° on the solar equator. This allows us to compute possible directions for the longitude of the ascending node of pl9 on the ecliptic plane.

Once we know the inclinations and longitudes of the ascending node of pl9 and also the inclination and ascending node of the solar equator with respect to the ecliptic, we can, with a couple of rotations, compute the longitude of the ascending node of pl9 on the ecliptic. Figures 7 and 8 already suggest that pl9's longitude of node will be constrained in a 180° range. On the ecliptic, Figure 9 shows the frequency of possible Ω's of pl9 for four possible I_9. All masses of pl9 from $2\times10^{-5}M_\odot$ to $5\times10^{-5}M_\odot$ are included in these plots. The vertical lines depict the range of Ω's determined by Batygin & Brown (2016; 113° ± 13°). Still, for $I_9=30^\circ$, Figure 10 shows the semimajor axis and eccentricity of pl9 whose Ω falls inside the range predicted by Batygin & Brown (2016).

We see that our approach does not constrain very well the longitude of the ascending node of pl9, but our determination usually includes Batygin & Brown's (2016) prediction based on the longitude of the ascending nodes of the distant TNO's. Interestingly, we have a better match for $I_9 > 45°$. For $I_9 = 25°$ and lower, we do not obtain any overlapping with the range of node longitudes from Batygin & Brown's (2016) work. For $I_9 = 30°$, we have compatibility with Batygin & Brown (2016) only for $m_9 \gtrsim 4 \times 10^{-5} M_\odot (\sim 13.3 M_\oplus)$. This seems to indicate that pl9's inclination cannot be much smaller than 30°, and, if so, it needs a mass of the order of $5 \times 10^{-5} M_\odot (\sim 17 M_\oplus)$, somewhat larger than the $10 M_\oplus$ usually assumed. This result does not match Malhotra et al. (2016), who give two choices for the pair I_9 and Ω_9, which are (18°, 101°) and (48°, 355°). The higher inclination is associated with a longitude of the node that cannot explain the tilt of the giant planets relative to the solar equator (see Figure 9).

It must be noted that when we refer to pl9's inclination, we mean its initial inclination with respect to the solar equator plane, which coincided with iv4. The final pl9 inclination with respect to the ecliptic, which should be compared with the current pl9's inclination, will vary a little from the initial reference inclination. For instance, for the case where $I_9 = 30°$, the final pl9's inclination with respect to the ecliptic will vary in a range from 27.°3 to 37.°2. If we restrict to the Ω's constrained by Batygin & Brown (2016), this range shrinks to 29.°7–33.°2.

4. CONCLUSIONS

Some ideas had been put forward to possibly explain the inclination of the invariant plane of the known planets relative to the solar equatorial plane (Batygin et al. 2011), but in view of the convincing case presented in Batygin & Brown (2016) for the existence of pl9, it is quite natural to suppose that such a tilt was caused by a slow precession of iv4 around the total angular momentum vector of the solar system (including pl9). In this paper, we constrained possible masses and orbital elements for pl9 that can account for the present tilt of iv4 with the solar equator. Our results are usually compatible with those of Batygin & Brown, (2016) and Brown & Batygin (2016) though with somewhat larger eccentricities. We also determine a range of possible longitudes of the ascending node for pl9 which often overlaps with the range given in Batygin & Brown (2016) except for smaller masses and inclinations of pl9. For instance, for $I_9 = 30°$, we need a mass larger than $\sim 4 \times 10^{-5} M_\odot \sim 13 M_\oplus$ to match the range of the longitudes of the ascending node for pl9 proposed by Batygin & Brown (2016).

R.D. acknowledges support provided by grants #2015/18682-6 and #2014/02013-5, São Paulo Research Foundation (FAPESP) and CAPES.

After the submission of this paper, we learned that Bailey et al. (2016) and Lai (2016) had also submitted similar works arriving at similar conclusions simultaneously. Thus, these works, providing consistent conclusions, have been done in parallel and independently.

REFERENCES

Adams, F. C., Proszkow, E. M., Fatuzzo, M., & Myers, P. C. 2006, ApJ, 641, 504
Bailey, E., Batygin, K., & Brown, M. E. 2016, AJ, 152, 126
Batygin, K., & Brown, M. E. 2016, AJ, 151, 22
Batygin, K., Morbidelli, A., & Tsiganis, K. 2011, A&A, 533, A7
Beck, J. G., & Giles, P. 2005, ApJL, 621, L153
Beust, H. 2016, A&A, 590, L2
Brasser, R., Duncan, M. J., & Levison, H. F. 2008, Icar, 196, 274
Brown, M. E., & Batygin, K. 2016, ApJL, 824, L23
Fienga, A., Laskar, J., Manche, H., & Gastineau, M. 2016, A&A, 587, L8
Gomes, R. S., Matese, J. J., & Lissauer, J. J. 2006, Icar, 184, 589
Gomes, R. S., Soares, J. S., & Brasser, R. 2015, Icar, 258, 37
Holman, M. J., & Payne, M. J. 2016, AJ, 152, 94
Izidoro, A., Morbidelli, A., Raymond, S. N., Hersant, F., & Pierens, A. 2015, A&A, 582, A99
Lai, D. 2016, arXiv:1608.01421
Madigan, A.-M., & McCourt, M. 2016, MNRAS, 457, L89
Malhotra, R., Volk, K., & Wang, X. 2016, ApJL, 824, L22
Murray, C. D., & Dermott, S. F. 1999, Solar System Dynamics (Cambridge: Cambridge Univ. Press)
Souami, D., & Souchay, J. 2012, A&A, 543, A133
Trujillo, C. A., & Sheppard, S. S. 2014, Natur, 507, 471